



HAL
open science

Ready to dive? Early constraints help juvenile southern elephant seals (*Mirounga leonina*) acclimatize to aquatic life

Laura Charlanne, Fabrice Bertile, Alexandre Geffroy, Lea Hippauf, Isabelle Chery, Sandrine Zahn, Christophe Guinet, Erwan Piot, Jérôme Badaut, André Ancel, et al.

► **To cite this version:**

Laura Charlanne, Fabrice Bertile, Alexandre Geffroy, Lea Hippauf, Isabelle Chery, et al.. Ready to dive? Early constraints help juvenile southern elephant seals (*Mirounga leonina*) acclimatize to aquatic life. *Journal of Experimental Biology*, 2025, 228 (6), <10.1242/jeb.249813>. <hal-05376841>

HAL Id: hal-05376841

<https://hal.science/hal-05376841v1>

Submitted on 21 Nov 2025

HAL is a multi-disciplinary open access archive for the deposit and dissemination of scientific research documents, whether they are published or not. The documents may come from teaching and research institutions in France or abroad, or from public or private research centers.

L'archive ouverte pluridisciplinaire **HAL**, est destinée au dépôt et à la diffusion de documents scientifiques de niveau recherche, publiés ou non, émanant des établissements d'enseignement et de recherche français ou étrangers, des laboratoires publics ou privés.



HAL Authorization

1 **Ready to dive? Early constraints help juvenile southern elephant seals (*Mirounga leonina*)**
2 **acclimatize to aquatic life**

3 Laura Charlanne¹, Fabrice Bertile^{1,2}, Alexandre Geffroy^{1,2}, Lea Hippauf³, Isabelle Chery¹, Sandrine Zahn¹,
4 Christophe Guinet⁴, Erwan Piot^{3,5}, Jérôme Badaut³, André Ancel¹, Caroline Gilbert^{5,6}, Audrey Bergouignan¹.

5
6 ¹Université de Strasbourg, CNRS, IPHC UMR 7178, 67000 Strasbourg, France

7 ²Proteomics French Infrastructure, FR2048, ProFI, Strasbourg 67000, France;

8 ³CNRS UMR 5536, Université de Bordeaux, 33076 Bordeaux, France

9 ⁴Centre d'Études Biologiques de Chizé, UMR 7372 CNRS/Université de La Rochelle, 79360 Villiers-en-Bois,
10 France.

11 ⁵UMR 7179, CNRS/MNHN, Laboratoire MECADEV, 1 avenue du petit château, 91400, Brunoy, France

12 ⁶Ecole Nationale Vétérinaire d'Alfort, 7 avenue du Général de Gaulle, 94704 Maisons-Alfort, France

13 *Corresponding author: laura.charlanne@iphc.cnrs.fr

14

15 **Abstract**

16 Breath-holding foraging implies different adaptations to limit oxygen (O₂) depletion and maximize foraging time.
17 Physiological adjustments can be mediated through O₂ consumption, driven by muscle mitochondria, which can
18 also produce reactive oxygen species during reoxygenation. Southern elephant seals spend months foraging at sea,
19 diving for up to one hour. Pups transition abruptly to aquatic life after a post-weaning period, during which they
20 fast and progressively increase their activity, making this period critical for the development of an adaptive
21 response to oxygen restriction and oxidative stress. We compared the functional capacity of a swimming muscle in
22 5 recently weaned and 6 adult female southern elephant seals. High-resolution respirometry was employed to
23 examine muscle mitochondrial respiratory capacity and differences in protein and gene expressions of the main
24 regulatory pathways were determined using LC-MS/MS and RT-PCR, respectively. Oxidative damages were
25 measured in the plasma. Juveniles have higher mitochondrial coupling efficiency compared to adults probably as a
26 response to growth and important physical activity reported during the post-weaning. There were no differences
27 in oxidative damage, but the adults had a higher level of antioxidant defenses. Both hypoxia and oxidative
28 response pathways appeared less activated in the juveniles. This study highlights the differences in muscle
29 metabolism and the likely adaptive response to hypoxia and oxidative stress between juveniles and adult south
30 elephant seals. It also suggests that early constraints such as fasting, physical activity, and short-term low O₂ partial
31 pressure exposure could contribute to immediate and long-term responses and to acclimatize juveniles to aquatic
32 life.

33

34 Keywords : diving – hypoxia – oxidative stress – acclimatization – post-weaning

35

36 **Summary statement**

37 This study suggests that the post-weaning period contributes to acclimatizing juvenile southern elephant seals to
38 aquatic life and the associated physiological constraints (limited O₂ supply and oxidative stress).

39 **INTRODUCTION**

40

41 Diving mammals are regularly exposed to oxygen (O₂) restriction, performing prolonged foraging dives in
42 apneic conditions (Elsner and Gooden, 1983; Kooyman, 2012; Meir et al., 2009; Qvist et al., 1986;
43 Ridgway et al., 1975). Breath-holding foraging implies increased physical activity despite the decline in
44 O₂ availability, which requires physiological adjustments for optimal O₂ consumption, such as peripheral
45 vasoconstriction, blood flow redistribution, or changes in mitochondrial efficiency, the cellular organelle
46 responsible for oxidative phosphorylation (van den Berg et al., 2011). Prolonged diving is also associated
47 with the generation of reactive oxygen species (ROS) and oxidative stress. During ischemia, superoxide
48 radical are generated through the activation of pro-oxidant enzymes such as NADPH oxidase (Brookes et
49 al., 2004; Granger, 1988; Granger and Kvietys, 2015; McCord, 1985). In addition, ROS are produced via
50 reverse electron transport at mitochondrial complex I during reperfusion (Chouchani et al., 2016). ROS
51 production and the associated biochemical damage increase with age. In parallel, a loss of function of
52 the antioxidant enzymes is noted. This raises the question of how diving mammals cope with the
53 alternation of low O₂ availability during apneas and reoxygenation after apneas and whether these
54 adaptations are influenced by age.

55 Several studies have focused on physiological adaptations to low oxygen availability and / or
56 oxidative stress in diving mammals. Previous studies on seals reported reduced cardiac output and
57 blood flow redistribution toward obligatory oxygen-dependent tissues during the dives (Elsner, 1999;
58 Kooyman and Ponganis, 1998; Lavigne et al., 1986). Massive oxygen stores, with 28% being in the
59 muscles, have also been noted (94 ml O₂ kg⁻¹, i.e., four times more than in humans), along with
60 physiological and behavioral adaptations to minimize oxygen depletion (Blix, 2018; Davis, 2014). Also,
61 seals have mechanisms that limit oxidative damage in plasma, tissues and red blood cells. For instance,
62 they are known to possess higher glutathione (GSH) levels than terrestrial mammals, and a rapid
63 upregulation of genes involved in GSH metabolism in their endothelial cells was noticed during hypoxia
64 exposure (Allen et al., 2024). Consequently, they exhibit lower levels of oxidative damage in their
65 tissues, including muscles (Murphy and Hochachka, 1981; Vázquez-Medina et al., 2006; Vázquez-Medina
66 et al., 2007; Wilhelm Filho et al., 2002; Wright et al., 2020; Zenteno-Savín et al., 2002). Muscle
67 mitochondrial adaptations were also investigated in extreme divers such as the northern elephant seal
68 (NES, *Mirounga angustirostris*). An acclimatization to the acute and repeated exposures of long breath-
69 hold exercises was shown in adults, characterized by an increased efficiency in coupling phosphorylation
70 (Chicco et al., 2014). The molecular pathways responsible for adaptations to low oxygen availability and
71 oxidative stress are also well-identified. Low partial O₂ pressure triggers the hypoxia adaptive response
72 through HIF-1 α , a transcription factor involved in angiogenesis, erythropoiesis, and myoglobin
73 production, helping in optimizing oxygen stores, redistribution, and consumption. On the other hand,

74 the transcription factor erythroid 2-related factor 2 (Nrf2) contributes to the activation of several
75 antioxidant enzymes. Both HIF-1 α and Nrf2 have been implicated in the seal's protection against apnea-
76 induced hypoxemia and ischemia/reperfusion (Johnson et al., 2004; Johnson et al., 2005; Vázquez-
77 Medina et al., 2011c). For instance, HIF-1 α and Nrf2 levels increased after a voluntary submersion in NES
78 (Vázquez-Medina et al., 2011c) or weddell seals (Murphy and Hochachka, 1981).

79 The ontogenesis of physiological adaptations to aquatic life in air-breathing mammals remains
80 unclear. Juveniles of many phocid species undergo a post-weaning period, fasting for several weeks,
81 before an abrupt transition to aquatic life. During this period, juveniles progressively increase their
82 physical activity and at-sea movements, making the post-weaning critical in the development of diving
83 abilities and adaptive response to low O₂ availability and oxidative stress (Noren et al., 2005; Prewitt et
84 al., 2010; Somo et al., 2015; Thorson and Le Boeuf, 2023; Vázquez-Medina et al., 2011b). An increase in
85 myoglobin abundance and maturation of the antioxidant system was already reported in juvenile
86 weddell seals (*Leptonychotes weddellii*), hooded seals (*Cystophora cristata*), and northern elephant seals
87 (NES, *Mirounga angustirostris*) (Geiseler et al., 2013; Moore et al., 2014; Vázquez-Medina et al., 2011a;
88 Vázquez-Medina et al., 2011b). However, underlying mechanisms and molecular pathways of the
89 ontogenetic development of diving abilities during this period remain unclear.

90 Southern elephant seals (SES, *Mirounga leonina*) spend months in the sea to feed, diving for up to
91 one hour, reaching depths of up to 1,000 m (Hindell et al., 1991; Slip et al., 1994). General physiological
92 adjustments are already described in NES, (Davis, 2014; Meir et al., 2009), but little is known about SES
93 which remain in a polar environment. Moreover, few studies have investigated both mitochondrial
94 performance and adaptive muscular and systemic responses to oxidative stress. As many other phocid
95 species, pups abruptly transition to aquatic life after a 3 to 4 weeks post-weaning fast on land before
96 leaving for their first trip to sea. This period is particularly costly for the juveniles as they progressively
97 increase their physical activity and at-sea movements (Piot et al., 2024). The combination of costly
98 events during the post-weaning period, the abrupt transition, and the ability of juvenile SES to perform
99 extreme dives make them good model species for studying this post-weaning period as preconditioning,
100 and the ontogenesis of physiological adaptations to O₂ restriction and oxidative stress.

101 The aim of this study was to compare the metabolic capacity of the swimming muscle in pups and
102 adult SES to help understanding the ontogenesis of the adaptations to the hypoxic living conditions.
103 High-resolution respirometry was employed to examine differences in muscle respiratory capacity
104 between the two groups. We assessed protein and gene expression differences on the same tissue using
105 liquid chromatography–mass spectrometry (LC-MS/MS) and gene expression measurements,
106 respectively. Indices of oxidative stress were measured in their plasma by quantifying lipid peroxidation
107 (isoprostanes, 8-isoPGF_{2a}) and protein oxidation (protein carbonyls, PC). We hypothesized that adults
108 would display greater mitochondrial efficiency than juveniles that had not yet been regularly exposed to

109 O₂ restriction and oxidative stress. We further assumed that the adaptive response to hypoxia and
110 oxidative stress would increase in adults, resulting in no difference in oxidative damage. As juveniles
111 remain physically active while fasting during this period, we thought they would show an upregulation
112 of mitochondrial biogenesis and metabolic pathways to meet the energetic demand they face on land,
113 which could contribute to increasing their adaptive response to physiological constraints they will face
114 later in life.

115

116 **MATERIALS AND METHODS**

117

118 **Data collection and analysis**

119 **Animal Sampling**

120 All scientific procedures were approved by the Ethics Committee of the French Polar Institute and the
121 French Ethics Committee (Cometh #32407-2021071212163407 v2) and followed the ARRIVE guidelines
122 (Sert et al., 2020). The study was conducted in 2022, from late October to mid-November, in Port-Aux-
123 Français (49°34'S, 70°21'E) in the Kerguelen Archipelago. Lactating adult females at the end of the
124 weaning period to avoid disturbance (N = 6) and juvenile females of approximately 5–6 weeks old during
125 the post-weaning period (N = 5) were sampled. All individuals remained on land fasting for 2 (juveniles)
126 to 3 weeks (adults). Females were lactating and strictly remained on land. Juveniles were on the beach
127 with the opportunity to play and swim in the sea. Animals were anesthetized with an initial dose of
128 tiletamine and zolazepam (Zoletil® 100) via intramuscular injection. They were measured and weighted,
129 and skeletal muscle biopsy and blood samples were collected, as described below.

130

131 **Muscle biopsy and blood sampling**

132 We performed a surgical biopsy of a swimming muscle (*longissimus dorsi*). During the surgical
133 procedure, anesthesia was maintained by successive injections of tiletamine and zolazepam (Zoletil®
134 100) into the extradural vein every five to ten minutes. The biopsy area was sterilized using iodinated
135 povidone 7.5% surgical scrub and iodinated povidone 10% solution (Vétédine®). Subsequent
136 subcutaneous administration of local anesthesia (1% lurocaïne®) was made before making a small
137 incision. Non-traumatic Mayo scissors were used to break adipose tissue until it reached the muscle
138 layer. An 8-mm biopsy cannula was introduced, and two muscle samples of approximately 30 mg each
139 were taken. One was placed into ice-cold BIOPS buffer (pH 7.1) containing 10 mM Ca²⁺-EGTA, 0.1 μM
140 free calcium, 20 mM taurine, 50 mM K-MES, 0.5 mM DTT, 6.56 mM MgCL₂, 5.77 mM ATP, and 15 mM
141 phosphocreatine until processing for mitochondrial respiration experiments within the following hour;
142 the other was placed into RNeasy lysis buffer and frozen at -20°C for later analysis. A simple interrupted
143 cutaneous suture with PDS® II D3T monofilament absorbable (2-0, 3/8, 24 mm; Ethicon) was made to

144 stitch the incision. The wound was cleaned with iodinated povidone 10% solution (Vétédine®) and
145 protected with an aluminum healing spray (Alumisol®). Postoperatively, the animals received an
146 intramuscular (IM) injection of both antibiotics (Penicillin, Streptomycin, Shotapen®, 13 mg/kg, and 16
147 mg/kg, respectively, without exceeding 12 mL per injection) and a non-steroidal anti-inflammatory drug
148 (Meloxicam, Metacam®, 0.5 mg/kg). The whole capture and surgical procedure lasted less than one
149 hour. After the biopsy, animals were monitored until complete voluntary locomotion was regained.
150 Blood samples were collected directly in the extradural vein in EDTA tubes after intramuscular
151 anesthesia. The tubes were centrifuged for 5 min at 4,000 rpm, and the plasma was pipetted into an
152 airtight vial and stored at -20°C until shipping and then at -80°C.

153

154 **High-resolution respirometry**

155 **Tissue preparation**

156 Muscle fiber bundles were selected from biopsies maintained in ice-cold BIOPS and mechanically
157 separated in a petri dish on ice. Adipose and connective tissue were removed using fine forceps under a
158 dissecting microscope. Teased fiber bundles (2–4 mg) were transferred to BIOPS containing 50 µg.ml⁻¹
159 saponin for 30 min of membrane permeabilization and washing of intracellular substrates (Gnaiger,
160 2009). Permeabilized muscle fibers were washed in ice-cold MiR05 respiration buffer containing 0.5 mM
161 EGTA, 3 mM MgCl₂, 60 mM lactobionic acid, 20 mM taurine, 10 mM KH₂PO₄, 20 mM HEPES, 110 mM
162 sucrose, and 1 g/l fatty acid free-BSA and gently rocked for 10 min to wash out residual saponin.
163 Permeabilized fibers were blotted on Whatman filter paper to remove excess buffer, weighed, and
164 immediately placed in the oxygraph chambers containing MiR05 at 37°C for stabilization before the
165 respiration experiments described below.

166

167 **Respirometry**

168 High-resolution tissue respirometry was performed on permeabilized muscle fibers obtained from the
169 *longissimus dorsi* using an Oxygraph-2K (O2K) respirometer (Oroboros Instruments, Innsbruck, Austria).
170 All respirometry data were collected at 37°C less than 2 hours after sampling. Before each protocol, the
171 oxygen electrode for each chamber was calibrated using ambient air. Permeabilized muscle fibers were
172 introduced into the chamber before partially sealing the chamber with a stopper. As respiration was low
173 and a hyperoxygenated environment was not relevant in our model, we decided not to add oxygen
174 before starting the measurements. Two protocols were performed for each sample (Table 1).
175 Cytochrome C was used to assess mitochondrial membrane integrity. An increase in respiratory flux of
176 more than 10% following ADP titration is usually used as a threshold to indicate that compromised outer
177 mitochondrial membranes invalidated the respirometry measures for a given sample. One
178 measurement had a ratio between the respiratory flux after adding cytochrome c and ADP of 14% and

179 another of 21%. Because all the experiments were run by the same person, under the same conditions,
 180 and the respiration values were good, we decided to keep both experiments in the final analysis.

181

182 **Table 1. High-resolution respirometry protocols (A and B) and associated respiratory states for muscle**
 183 **fiber mitochondrial respiration experiments.**

184

Protocol components (in order of titration)	Respiratory state
A Palmitoyl-carnitine (0.04 mM) + malate (0.1 M)	LEAK; uncoupled respiration in the presence of long and short chain fatty acid concentration
Octanoyl-carnitine (0.2 mM)	
ADP (5 mM)	OXPHOS FA; Fatty acid stimulated respiration
Cytochrome c (0.01 mM)	CytC; Test of outer mitochondrial membrane integrity
Malate (5 mM) + Pyruvate (5 mM) + Glutamate (10 mM) + Succinate (10 mM)	OXPHOS CI+CII ; Complex I+II coupled respiration
Carbonylcyanide <i>p</i> -trifluoromethoxy-phenylhydrazone (FCCP, 0.001 mM)	MAX CI+CII; Maximal uncoupled Complex I and II capacity
Rotenone (0.005 mM)	MAX CII; Maximum uncoupled Complex II capacity
Malonate (5 mM) + Antimycine (0.0025 mM)	RESIDUAL; Residual oxygen concentration
B Pyruvate (5mM) + Malate (5 mM)	LEAK; Complex I uncoupled respiration
Glutamate (10 mM)	
ADP (5 mM)	OXPHOS CI; Complex I coupled respiration
Cytochrome c (0.01 mM)	CytC; Test of outer mitochondrial membrane integrity
Succinate (10 mM)	OXPHOS CI+CII ; Complex I+II coupled respiration
Carbonylcyanide <i>p</i> -trifluoromethoxy-phenylhydrazone (FCCP, 0.001 mM)	MAX CI+CII; Maximal uncoupled Complex I and II capacity
Rotenone (0.005 mM)	MAX CII; Maximum uncoupled Complex II capacity
Malonate (5 mM) + Antimycine (0.0025 mM)	RESIDUAL; Residual oxygen concentration

185

186 We assessed SES *longissimus dorsi* skeletal muscle oxygen consumption *ex vivo* in primary respiratory
 187 states, including measurement of LEAK respiration, OXPHOS, and MAX respiratory flux through
 188 respiratory complexes I and II (CI+CII). Uncoupled MAX respiration reflects the maximum mitochondrial

189 respiratory flux (Votion et al., 2012). OXPHOS respiratory capacity represents the portion of MAX
190 capacity composed of both the respiratory flux coupled to mitochondrial oxidative phosphorylation
191 through ATP synthase and non-coupled LEAK respiration. Steady-state respiratory values were corrected
192 for baseline respiratory chamber oxygen flux determined at the beginning of each protocol. Oxygen flux
193 was monitored in real-time following standardized instrumental and chemical background calibrations
194 using Datlab software 7.4.0.4 (Oroboros Instruments).

195

196 **Protein and RNA extraction**

197 Muscle tissues were processed to extract protein and RNA simultaneously (Khudyakov et al., 2022).
198 Muscle tissue (~30 mg) was isolated from RNA later while frozen and crushed. The tissue was processed
199 using 1 ml of Trizol. RNA and proteins were separated through a chloroform-phase extraction. Proteins
200 were precipitated from the organic phase using isopropanol, and pellets were washed with 0.3 mol/l
201 guanidine hydrochloride in 95% ethanol and stored at -80°C until further processing. RNA was cleaned
202 using RNeasy Mini Kit (Qiagen®). The amount and purity of RNA were measured with a Nanodrop and
203 RNA stored at -80°C until further analysis.

204

205 **Protein levels – quantitative mass spectrometry-based analysis**

206 **Muscle proteome analysis using DIA-based nanoLC-MS/MS**

207 This method provides a robust method for large-scale, high-throughput protein analysis.

208 Detailed methods are provided in the Supplemental Materials (Supplementary Methods). From the
209 protein extracts of elephant seal muscles, a reference sample comprising an equal protein quantity of all
210 protein extracts was made for quality assessment of LC-MS/MS. Individual samples and the reference
211 sample were electrophoresed using SDS-PAGE gels. A stacked protein band, as well as the part of the gel
212 above this band, were excised from the gel, and proteins were in-gel reduced, alkylated and then
213 digested at 37°C overnight with trypsin (Promega). A set of reference peptides (Indexed Retention Time
214 [iRT] Kit, Biognosys AG) was added to the resulting peptides to allow the stability of instrument
215 performance to be measured for QC purposes. Samples were analyzed on a nano-ultraperformance LC
216 system (nanoElute 1) coupled to a hybrid trapped ion mobility spectrometry – quadrupole time of flight
217 mass spectrometer (TimsTOF Pro 2) (Bruker Daltonics). The TimsTOF Pro 2 mass spectrometer was
218 operated in data-dependent acquisition (DDA)-parallel accumulation-serial fragmentation (PASEF) mode
219 (Meier et al., 2018) or repeated injections of the reference sample, allowing the stability of the system
220 to be assessed throughout the experiment and to optimize the method used in data-independent
221 acquisition PASEF (diaPASEF) mode (Meier et al., 2020) for differential analysis of the muscle proteome
222 between adult and juvenile individuals. Mass spectrometry data acquired in DDA-PASEF mode were
223 processed using Maxquant v2.4.7.03 (Tyanova et al., 2016), whereas those acquired in diaPASEF mode

224 were processed using directDIA implemented in Spectronaut v18 (Lou et al., 2023). The protein
225 database that we used was obtained from the latest annotation of the *Mirounga leonina* (TaxID 9715)
226 genome in Refseq (Refseq Assembly accession GCF_011800145.1; Assembly Name KU_Mleo_1.0). For
227 DDA-PASEF data, the false discovery rate (FDR) was set to 1% for both peptide and protein spectrum
228 matches. For diaPASEF data, identification was performed using a mutated method for decoy generation
229 with a dynamic limit strategy, and the precursor Qvalue cutoff was set to 1% and the protein Qvalue
230 cutoff to 1% (experiment and run).

231 Regarding the quantification of DDA-PASEF data, normalization and protein abundance estimation were
232 performed using the label-free quantification (LFQ) option offered in MaxQuant (Cox et al., 2014).
233 Quantification of diaPASEF data was performed using Spectronaut (Lou et al., 2023), using only protein
234 group-specific peptides. The raw files from the analysis in DDA-PASEF mode of the repeated injections of
235 the reference sample were specified to create a hybrid library and analyse accurately diaPASEF data, for
236 which only the proteins quantified in at least four individuals per group were retained. The mass
237 spectrometry proteomics data have been deposited to the ProteomeXchange Consortium
238 (<http://proteomecentral.proteomexchange.org>) via the PRIDE partner repository (Perez-Riverol et al.,
239 2022) with the dataset identifier PXD048683.

240 Data indicated a good reproducibility of quantitative measurements in DDA-PASEF, with a mean CV of
241 19% for all LFQ values determined from the repeated analysis of this reference sample. QC-related
242 measurements also showed that HPLC performance remained good and stable throughout the whole
243 experiment, with a median coefficient of variation of 0.67% concerning retention times of all iRT
244 peptides when considering all injections.

245

246 **Functional enrichment and pathway analysis**

247 Hierarchical clustering of proteomics data was performed using Cluster V3.0 software (de Hoon et al.,
248 2004), with the following parameters: median centering and normalization of genes for adjusting data
249 and centroid linkage clustering for both genes and arrays. A dendrogram was generated and viewed
250 using the Java Treeview V1.3.3 program (Page, 1996).

251 To enable automatic functional annotation of elephant seal proteins, we first identified their human
252 homologs using BLAST searches (FASTA program v36; downloaded from
253 http://fasta.bioch.virginia.edu/fasta_www2/fasta_down.shtml) against Swissprot-derived human
254 protein sequences (20 427 entries, November 2023), combined with a careful examination of protein
255 names and gene symbols. Only the best hits were retained, and inspection of the relevance of the
256 matches one by one led us to reject only three entries out of the 1,708 quantified proteins. Functional
257 annotation enrichment analysis was then performed using human protein identifiers from the list of
258 differentially expressed proteins, including present/absent cases, using the desktop version of DAVID

259 (Ease V2.0) and an updated (November 2023) version of Gene Ontology (GO) and Kyoto Encyclopedia of
260 Genes and Genomes (KEGG) databases generated using the MSDA software (Carapito et al., 2014). All
261 the Swissprot-derived human protein sequences used previously for BLAST searches were used here as
262 the enrichment background. Enriched GO terms were filtered by only considering those with a
263 Benjamini p-value lower than 0.05 and a fold enrichment higher than 1.5. Enriched GO terms were
264 grouped together into broad functional categories, which were then considered as enriched broad
265 functions. KEGG mapping tools (Kanehisa and Sato, 2019) were used for complementary biological
266 interpretation of our proteomics dataset.

267

268 **Muscle fiber typing**

269 The proteome analysis allowed us to specify the fiber type profile of our samples through myosin
270 isoform identification. Results are expressed as a percentage of the total myosin isoforms detected.
271 Type I (slow oxidative fibers) were identified through myosin isoform Myh7 (Talmadge and Roy, 1993),
272 and Type IIa (fast oxidative-glycolytic fibers) through myosin isoform Myh2 (Schiaffino and Reggiani,
273 1994). No Type IIb (fast glycolytic fibers, isoform Myh4) were found in our samples.

274

275 **Gene expression – real-time reverse-transcription PCR**

276 Five hundred nanograms of RNA were reverse transcribed using the Primescript RT Reagent kit (TAKARA
277 BioEurope SAS) according to the manufacturer's instructions. cDNAs were used to perform real-time RT-
278 PCRs. We investigated different genes involved in metabolic response to hypoxia, oxidative stress, and
279 exercise. We selected a complex I subunit gene expression (NDUFS3), two genes involved in protein
280 turnover (mTOR and Trim63), one related to muscular adaptive response to exercise and oxidative
281 stress (PGC1 α), one involved in lipogenesis (ACCb), and the two transcription factors HIF-1 α and NRF2.
282 Real-time PCRs were made using primers specially designed for the study (Table S1). Amplification (45
283 cycles of denaturation at 95 °C for 15 s, annealing at 60 °C for 15 s, and extension at 72°C for 45 s) was
284 monitored using SYBR green (GoTag[®] qPCR kit, Promega, France). Three housekeeping genes were
285 tested: actin (ACT), glyceraldehyde-3-phosphate dehydrogenase (GAPDH), and succinate dehydrogenase
286 complex flavoprotein subunit A (SDHA). GeNorm software was used to choose the best internal control,
287 and the combination of ACT/SDHA was kept (M = 0.029). Fold change was calculated by the Pfaffl
288 method (Pfaffl, 2001). All results were obtained in duplicates (CV < 0.5%).

289

290 **Plasma measurements**

291 Plasma levels of 8-isoprostanes (8-isoPGF2 α) were measured in duplicate using a competitive EIA assay
292 kit (Cell BioLabs, San Diego, CA, USA). Plasma protein carbonyls (PC) were also measured in triplicate
293 using commercially available ELISA kits (Cell BioLabs, San Diego, CA, USA,) (Vázquez-Medina et al., 2010).

294 Total protein content was measured using the BCA Protein Assay (ThermoFischer Scientific, Rockford,
295 USA).

296 **Statistical analysis**

297 The normality of the data distribution and homoscedasticity were checked using the Shapiro-Wilk test
298 ($P > 0.01$) and Bartlett test ($P > 0.01$), respectively, in the R software environment (v4.2.2) (R Core Team).
299 For the LC-MS/MS analysis, protein abundances in juvenile and adult individuals were compared using
300 Welch two-sample t-tests ($P < 0.05$ required to conclude on differential expression levels). Of the
301 differentially expressed proteins ($P < 0.05$), subsequent analyses and interpretations took into account
302 only those whose levels differed by at least 40% between the two groups of elephant seals. Results are
303 expressed as mean \pm standard error unless otherwise specified. Because of non-normality and
304 heteroscedasticity, high-resolution respirometry, gene expression and oxidative damage results were
305 compared using Wilcoxon tests.

306

307 **RESULTS**

308

309 The mean body mass of juvenile females SES ($N = 5$) was 103.5 ± 6.6 kg, with a mean body length of 140
310 ± 4.6 cm. Adult females ($N = 6$) were sampled at the end of the lactation period with a mean body mass
311 of 294 ± 19.8 kg, and a body length of 247.5 ± 8.8 cm.

312

313 **High-resolution respirometry**

314 Muscle mass-specific O_2 fluxes in juveniles and adults are illustrated in Figure 1, based on the sequential
315 addition of each protocol component as described in Table 1. We found no differences in O_2 fluxes
316 between juveniles and adult SES in the presence of either carbohydrate-related or fatty acid-related
317 substrates, indicating a general similarity in mitochondrial functional capacity between the two stages of
318 life. In both protocols, the addition of FCCP (MAX_{Cl+ClI}) did not increase O_2 fluxes, indicating that the
319 muscle mitochondria of juvenile and adult SES were working at their maximal capacity. However, we
320 observed a greater OXPHOS coupling control factor (OXPHOS-LEAK/OXPHOS) in the presence of fatty
321 acids in the juveniles (0.576 ± 0.030) compared to the adults (0.377 ± 0.090 , Wilcoxon test, $W = 3$, $p =$
322 0.03 , Figures 1A and 1C). In adults, LEAK was higher in the presence of fatty acids than carbohydrate-like
323 substrates (5.68 ± 0.75 vs 2.18 ± 0.75 , Wilcoxon test, $W = 3$, $p = 0.02$). As our LEAK values were very low,
324 we could not use residual oxygen consumption as a correction factor for all mitochondrial respiratory
325 rates; we are likely at the limit of the sensitivity of the machine. We kept the raw values and reported
326 the residuals (Figure 1).

327

328 **LC-MS/MS**

329 **Southern elephant seals' muscle proteome changes between juveniles and adults**

330 We identified 2,065 proteins in muscle, of which 1,708 could be accurately quantified, and we found
331 significant age effects for the abundance of 270 muscle proteins, with 128 of them being increased and
332 142 decreased in juvenile SES compared with adults (Figure 2A, Table S2). Three proteins associated
333 with protein turnover and small-molecule transport across the mitochondrial membrane were well
334 detected in adults but remained below our detection limit for juveniles. The same applies to eight
335 proteins related to cell integrity and mobility, cell matricial components, and the immune system, which
336 were only detected in juvenile samples.

337 The most significant differences observed in muscle protein levels were in the mitochondrial pathways
338 (Figure 2B) with up-regulation in juveniles (Figure 3). NADH dehydrogenase and cytochrome c oxidase of
339 the respiratory electron chain were up-regulated, but there was no difference in citrate synthase. The
340 expression of several proteins involved in the TCA cycle (pyruvate dehydrogenase kinase, fumarate
341 hydratase, and isocitrate dehydrogenase) and fatty acid β -oxidation (ACADM, ECI1, and HCDH) was
342 increased in juveniles. Mitochondrial transporters were also increased in juveniles (M2OM for
343 malate/alpha-oxoglutarate, acylglycerol kinase, and AGK for protein import), as well as mitochondrial
344 biogenesis and morphogenesis (identified by STML2, TMM11), and the energy cell sensor protein kinase
345 AMPK γ 1. No differences in glycolysis were, however, observed.

346 The expression of most of the proteins involved in oxidative defenses was lower in the muscle of the
347 juveniles, including catalase, superoxide dismutase (SOD1), peroxidase (PRDX), glutathione peroxidase 3
348 (GPx3), one glutathione transferase (GST), thioreductase (TRXR1), and glutathione reductase (GR). Only
349 two other GSTs (kappa and omega) were increased in juveniles. We found no difference in xanthine
350 oxidase, GPx1 and 4, SOD2 and SOD3, or glutathione synthetase. As expected, because such molecules
351 are generally expressed at low levels, Nrf2, the redox-sensitive transcription factor that controls the
352 expression of antioxidant genes, was not detected with mass spectrometry.

353 Proteins of the HIF-1 signaling pathway involved in the adaptive response to hypoxia were detected.
354 Although HIF1- α itself could not be detected, HIF1N, an HIF1- α inhibitor, was measured; no difference
355 was observed between the juveniles and adults. However, the expression of EGLN1, a cellular oxygen
356 sensor involved in hypoxia-influenced processes known to regulate the HIF1 signaling pathway, was
357 even less pronounced in juveniles.

358 Finally, we specified muscle fiber types (Type I or IIa) through myosin isoform identification. Both
359 juveniles and adults showed a similar high proportion of Type I fibers (60.9 ± 1.9 % and 67.6 ± 2.8 % ,
360 $p=0.09$). The proportion Type IIa were higher in juveniles but considerably low compared to Type I
361 (myosin-2 isoform, 1.4 ± 0.3 % in juveniles and 0.29 ± 0.05 % in adults, $p=0.02$).

362

363 **Gene expression**

364 Transcript levels were expressed relative to ACT/SDHA and reported in Table 2. Individual values are
 365 available in Table S3. We found an increase in gene expression of mitochondrial respiratory chain
 366 complex I in juveniles (higher NDUFS3). An up-regulation of the peroxisome proliferator-activated
 367 receptor- γ coactivator-1 α (PGC-1 α) was also noted in juveniles. Gene expression of both mTOR and
 368 Trim63, related to protein turnover, was increased in adults. No difference was observed between our
 369 groups for HIF-1 α , NRF2, and ACCb.

370

371 **Table 2: Gene expression in juvenile (N=5) and adult (N=6) female southern elephant seals.** Gene
 372 expression was evaluated by real-time RT-qPCR and normalized to the expression of the reference genes
 373 ACT/SDHA. Fold change was calculated by the Pfaffl method. All results were obtained in duplicates (CV
 374 < 0,5%). P values are indicated for the comparison of juvenile and adult southern elephant seal
 375 transcripts as determined by the Wilcoxon W-test. A positive fold change means an increased gene
 376 expression in juveniles compared to adults.

377

Gene	Fold change (juvenile / adults)	W	P value
NDUFS3	1.59	29	0.009
HIF-1 α	-1.10	12	0.662
NRF2	-1.13	12	0.662
ACCb	-1.24	4	0.051
PGC1a	2.28	29	0.009
mTOR	-1.45	2	0.017
Trim63	-2.83	2	0.017

378

379

380 Oxidative damages

381 Plasma contents of 8-isoPGF2a and protein carbonyls were measured as proxies of oxidative stress (Fig
 382 4). No difference was observed in either 8-isoPGF2a (juveniles: 171 \pm 19 ng/ml, adults: 213 \pm 10.9 ng/ml,
 383 Wilcoxon test, W = 7, p-value = 0.18) or protein carbonyls (juveniles: 6.0 \pm 0.3 nmol/mg, adults: 6.0 \pm 0.2
 384 nmol/mg, Wilcoxon test, W = 15, p-value = 1.0).

385

386 DISCUSSION

387 SES maintain significant levels of physical activity during deep dives despite limited O₂ availability
 388 (Hindell et al., 1991). This ability is supported by a suite of complex behavioral and physiological
 389 adaptations (Davis, 2014). The present experimental design compares the metabolic capacity of the
 390 swimming muscle in pups and adult SES. Although the single sampling of early-fasting juveniles does not
 391 allow us to conclude on the development of the antioxidant defenses and metabolic adjustments
 392 needed to cope with breath-hold diving, this study is the first in the southern species to shed light on
 393 the ontogenesis of metabolic adaptations to hypoxic conditions

394 Our results show an important proportion of Type I muscle fibers and a low one of Type IIa in
395 both groups, although more Type IIa were found in juveniles compared to adults. No Type IIb were
396 found in both groups. This is in line with the ontogenetic changes in muscle fibers along the post-
397 weaning already described in NES and weddell seals (Kanatous et al., 2003; Moore et al., 2014). This
398 suggests juveniles' muscle structure was close to adults' when the sampling occurred.

399

400 In this study, we found a higher OXPHOS coupling control factor in juveniles in the presence of
401 fatty acids, explained by a higher OXPHOS relative to LEAK capacity. This finding was supported by
402 proteomic data showing an increase of proteins involved in several mitochondrial metabolic pathways in
403 juveniles compared to adult females (beta-oxidation, citrate cycle, mitochondrial imports, and
404 biogenesis). The opposite was found in juvenile and adult male NES, which indicates that a higher
405 coupling control factor in adults was a mitochondrial adaptive response to diving (Chicco et al., 2014).
406 However, the OXPHOS coupling control factor is notably lower for fatty acids in our adult female SES
407 compared to the values reported by others in adult post-breeding male NES (0.3 *versus* 0.8) (Chicco et
408 al., 2014). In our study, the females were lactating, a physiological state associated with a dramatic
409 increase in energy demands for milk production. Consistent with this, studies in rats have reported a
410 reduction in fatty oxidation in skeletal muscles as a potential mechanism to spare fatty acids for milk
411 production (Gutgesell et al., 2009; Xiao et al., 2004). The reduced coupling efficiency observed in our
412 lactating female SES may therefore reflect an adaptative metabolic response to their energy-intensive
413 productive state.

414 Many lactating mammals increase their energy intake by 60–200% to meet the energy demand of milk
415 production (Gittleman and Thompson, 1988). In contrast, female elephant seals fast during the 3-week
416 nursing period, relying exclusively on fat stores (Crocker et al., 2001). In non-fasting and still-active
417 lactating mammals muscle mitochondrial activity typically remain unchanged (Favorit et al., 2021).
418 However, the limited energy availability in fasting female SES is associated with behavioral and
419 physiological adaptations, such as reduced physical activity. This contrasts with males, that expend
420 significant energy fighting during the breeding season, and growing juveniles that progressively increase
421 activity during the post-weaning period (Lavigne et al., 1986; Modig et al., 1997; Piot et al., 2024). These
422 differences could explain the higher mitochondrial coupling efficiency observed in our juvenile SES,
423 comparable to values reported in recently weaned juvenile NES (Chicco et al., 2014). This is supported
424 by previous studies showing increased PGC1 α gene expression and activation of the AMPK pathway in
425 skeletal muscle of juveniles – both being key drivers of the muscular adaptive response to exercise (Baar
426 et al., 2003; Tadaishi et al., 2011). These findings align with our observed up-regulation of mitochondrial
427 energetic pathways, consistent with earlier reports in juvenile NES (Piotrowski et al., 2021). Thus the
428 variations in mitochondrial coupling efficiency across groups may result primarily from differences in

429 activity levels. Additional evidence comes from studies focusing on molting, another prolonged and
430 energy-intensive on-land period. Molting female NES showed no changes in muscle respiratory capacity
431 before and after molting, despite undergoing prolonged caloric restriction (Wright et al., 2020).
432 However, emerging data suggest that SES females exhibit greater activity during molting than than
433 during lactation (Charlanne et al., 2024), challenging the assumption they fast strictly and remain on
434 land throughout the molting period. This highlights the importance of integrating behavioral monitoring
435 with physiological data to better understand the drivers and implications of metabolic adaptations in
436 this species.

437 Finally, the observed mitochondrial adaptations may also reflect the effect of fasting or hypoxia, as the
438 AMPK pathway is known to be up-regulated in response to both low energy availability and low oxygen
439 partial pressure (Mungai et al., 2011; Weir et al., 2017). Consequently, the changes in mitochondrial
440 function and energy metabolism observed in juveniles likely result from the combined effects of these
441 physiological constraints. Early exposure to energetically demanding conditions may activate pathways
442 and adaptations that prepare SES juveniles to cope with the constraints of prolonged, deep dives in
443 adulthood.

444 Our results also show a major contribution of CII to the electron transport chain. In both groups, either
445 through the use of substrate-like fatty acids or carbohydrates, CII accounts for 60 to 80% of the
446 respiratory ratio. The same finding was reported in juvenile and adult NES, but not in pups (Chicco et al.,
447 2014). CII was recently suggested to play a role in the development of the reserve respiratory capacity
448 (RRC), the difference between the maximum respiratory capacity and basal respiratory capacity, known
449 to increase supply when energy demand exceeds reserves (Pfleger et al., 2015). Indeed, CII can mediate
450 a synchronized increase of substrate entry into the citrate cycle and of the electron transport chain
451 activity, known as a potential source of RCC (Bourgeron et al., 1995). In that study, the authors
452 identified CII as a target of different metabolic sensors such as PDH and AMPK, maximizing the cellular
453 RCC and enhancing cell survival after hypoxia (Pfleger et al., 2015). Consequently, both juvenile and
454 adult SES could benefit from a high CII activation as they experience long fasting periods and/or hypoxia
455 exposure. This could explain the observed lower contribution of CII in pups that have not experienced
456 these challenges yet.

457 Taken together, these data highlight the critical role of mitochondrial respiratory plasticity in adapting to
458 energy imbalances and physiological constraints experienced by diving mammals during their time on
459 land.

460 Cellular and molecular responses involved in the seal's adaptations to low O₂ availability and
461 protection against ischemia/reperfusion are well described. HIF-1 controls the adaptive response to
462 hypoxia by stimulating many physiological responses, such as erythropoiesis, angiogenesis, or myoglobin
463 level (Johnson et al., 2004; Johnson et al., 2005; Vázquez-Medina et al., 2011c). No difference was found

464 in HIF-1 α gene expression between juveniles and adults, and HIF-1 α factor was not detected at the
465 protein level. However, the HIF pathway involves several molecular interactions likely responsible for
466 the degradation of HIF-1 α by intracellular proteases, highlighting the complex regulation of this adaptive
467 response. In our proteomic analysis, several markers involved in HIF-1 α pathway were down-regulated
468 in juveniles (HIF-N, EGLN1). This is consistent with a progressive increase in the diving performance and
469 aerobic capacity of adult muscles, as already reported in post-weaned seals (NES (Somo et al., 2015);
470 weddell seals (Kanatous et al., 2008); Antarctic fur seals (LaRosa et al., 2012)). An increase of HIF-1 α was
471 reported in NES pups from the seventh week of the post-weaning period (Soñanez-Organis et al., 2013).
472 Because our juveniles were sampled early during the post-weaning period, they may not have been yet
473 sufficiently exposed to short apnea episodes to stimulate this pathway.

474 The adaptive response to oxidative stress consists of upregulating antioxidant genes in response to
475 increased oxidant production, mediated through the Nrf2 transcription factor. An increase in antioxidant
476 defenses and Nrf2 abundance was previously reported in NES after a voluntary submersion (Vázquez-
477 Medina et al., 2011c). In our study, we could not detect Nrf2 at the protein level, and no difference in
478 Nrf2 gene expression was found. In contrast, we found that antioxidant defenses, such as SOD, PRDX,
479 Gpx, and catalase, were up-regulated in adults compared to juveniles. Similarly, markers of protein
480 turnover, such as mRNA levels of mTOR and Trim63, were higher in adults, potentially reflecting
481 mechanisms for the removal of oxidized soluble cell proteins (Rivett, 1985). This age-related increase in
482 muscle expression of antioxidant-related genes is consistent with previous findings reported in NES
483 (Crocker et al., 2016; Piotrowski et al., 2021) and likely reflects the more pronounced oxidative stress
484 experienced by adults. Despite these differences, we found no difference in oxidative damage to lipids
485 and proteins between groups (Fig 4) (Levine et al., 1994; Roberts and Morrow, 2000). These results align
486 with previous studies suggesting that seals experience minimal oxidative damage despite repeated
487 exposure to ischemia-reperfusion, likely thanks to robust antioxidant defenses (Murphy and Hochachka,
488 1981; Vázquez-Medina et al., 2006; Vázquez-Medina et al., 2011c; Wilhelm Filho et al., 2002; Wright et
489 al., 2020; Zenteno-Savín et al., 2002).

490 Finally, oxidative stress is also a direct consequence of prolonged fasting, as it is associated with
491 increased activity of xanthine oxidase, a pro-oxidant enzyme (Hille and Nishino, 1995). Moreover,
492 oxidative stress has been identified as a potential physiological cost of reproductive effort (Monaghan et
493 al., 2009; Speakman and Garratt, 2014). Supporting this, female NES exhibited elevated oxidative
494 damage to proteins after 4 weeks of lactation, accompanied by increased plasma xanthine oxidase,
495 catalase and GPX activity (Sharick et al., 2015). In our study, the females were 3 weeks into their
496 lactation fast, while the juveniles had been fasting for approximately 2 weeks. Therefore, the oxidative
497 damage and changes in antioxidant enzyme activity in this experimental design likely reflect not only the
498 impact of hypoxia exposure but also the combined physiological demands of fasting and lactation.

499

500 In summary, this study highlights muscle metabolism and functional capacity according to age
501 and constraints experienced by the animals. Muscle mitochondrial plasticity likely allows animals to
502 meet the energetic demand on land. Hypoxia adaptive response and maturation of the antioxidant
503 system are higher in adults, probably reflecting an adaptive response to regular constraints exposure.
504 These results suggest the combination of fasting, physical activity, and short-term low O₂ partial
505 pressure exposure could contribute to acclimatize juveniles to aquatic life. As young animals only
506 perform short at-sea travels and apneas compared to those during their first and subsequent long
507 offshore trips, a long post-weaning fast could be mostly required to activate these adaptations rather
508 than intense physical training to perform extreme dives. Further studies investigating both physiological
509 and behavioral adaptations during post-weaning, as well as diving behavior during their first year at sea,
510 may reveal additional information on the development of diving abilities and the impact of first-year at-
511 sea survival in this species.

512

513 LIST OF ABBREVIATIONS

514

EGLN1	Hypoxia-inducible factor prolyl hydroxylase 2
8-isoPGF2a	8-isoprostanes
GSH	Glutathione
GPx	Glutathione peroxidase
H ₂ O ₂	hydrogen peroxide
HIF-1 α	hypoxia inducible factor
Nox4	NADPH oxidase
Nrf2	NF-E2-related factor 2
PC	Protein carbonyls
PRDX	Peroxidase
SOD	Superoxide dismutase

515

516 Acknowledgements

517 We thank the Terres Australes et Antarctiques Françaises for logistic support and the fieldwork
518 volunteers who helped in surgical work (in alphabetic order: Jibril Azaymen, Lea Hippauf, Laurent Levy,
519 Florence Niemetzky, Erwan Piot, and Nathan Thenon). We also thank A. Stier, A. Charlot, and D. Roussel
520 for the help and suggestions in the data analysis.

521

522 Competing interest

523 The authors declare no competing or financial interests.

524

525 **Author contributions :**

526 C. G., A. B., A. A., and L. C. conceived and designed the overall study. L. C. and L. H. collected the data. A.

527 G. and F. B. made the LC-MS/MS analyses. S. Z. designed the primers and made the genomic analyses. L.

528 C. and I. C. performed the molecular analyses on oxidative damages. L. C. performed the statistical

529 analyses and drafted the manuscript. All authors reviewed and agreed on the content of the manuscript.

530

531 **Funding**

532 The present research project was supported by the Institut Polaire Français Paul-Emile Victor (IPEV

533 program 1201), two doctoral fellowships from the French Ministry of Higher Education and Research

534 and ANR (ANR HYPO2), and by French Proteomic Infrastructure (ProFI; ANR-10-INSB-08-03).

535

536 **Data and code availability:**

537 Data and R-code are available on figshare at [10.6084/m9.figshare.26403949](https://doi.org/10.6084/m9.figshare.26403949)

538

539 **References**

540

541 **Allen, K. N., Torres-Velarde, J. M., Vazquez, J. M., Moreno-Santillán, D. D., Sudmant, P. H. and**
542 **Vázquez-Medina, J. P.** (2024). Hypoxia exposure blunts angiogenic signaling and
543 upregulates the antioxidant system in endothelial cells derived from elephant seals.
544 *BMC Biol* **22**, 91.

545 **Baar, K., Wende, A., Jones, T., Marison, M., Nolte, L., Chen, M. H., Kelly, D. and Holloszy, J.**
546 (2003). Adaptations of skeletal muscle to exercise: Rapid increase in the transcriptional
547 coactivator PGC-1. *FASEB journal : official publication of the Federation of American*
548 *Societies for Experimental Biology* **16**, 1879–86.

549 **Blix, A. S.** (2018). Adaptations to deep and prolonged diving in phocid seals. *Journal of*
550 *Experimental Biology* **221**, jeb182972.

551 **Bourgeron, T., Rustin, P., Chretien, D., Birch-Machin, M., Bourgeois, M., Viegas-Péquignot, E.,**
552 **Munnich, A. and Rötig, A.** (1995). Mutation of a nuclear succinate dehydrogenase gene
553 results in mitochondrial respiratory chain deficiency. *Nat Genet* **11**, 144–149.

554 **Brookes, P. S., Yoon, Y., Robotham, J. L., Anders, M. W. and Sheu, S.-S.** (2004). Calcium, ATP,
555 and ROS: a mitochondrial love-hate triangle. *American Journal of Physiology-Cell*
556 *Physiology* **287**, C817–C833.

557 **Carapito, C., Burel, A., Guterl, P., Walter, A., Varrier, F., Bertile, F. and Dorselaer, A.** (2014).
558 MSDA, a proteomics software suite for in-depth Mass Spectrometry Data Analysis using
559 grid computing. *Proteomics* **14**,.

- 560 **Charlanne, L. M., Chaise, L., Sornette, D., Piot, E., McCafferty, D. J., Ancel, A. and Gilbert, C.**
561 (2024). Breaking the fast: first report of dives and ingestion events in molting southern
562 elephant seals. *Commun Biol* **7**, 1–12.
- 563 **Chicco, A. J., Le, C. H., Schlater, A. E., Nguyen, A. D., Kaye, S. D., Beals, J. W., Scalzo, R. L., Bell,**
564 **C., Gnaiger, E., Costa, D. P., et al.** (2014). High fatty acid oxidation capacity and
565 phosphorylation control despite elevated leak and reduced respiratory capacity in
566 northern elephant seal muscle mitochondria. *Journal of Experimental Biology*
567 jeb.105916.
- 568 **Chouchani, E. T., Pell, V. R., James, A. M., Work, L. M., Saeb-Parsy, K., Frezza, C., Krieg, T. and**
569 **Murphy, M. P.** (2016). A Unifying Mechanism for Mitochondrial Superoxide Production
570 during Ischemia-Reperfusion Injury. *Cell Metabolism* **23**, 254–263.
- 571 **Cox, J., Hein, M. Y., Lubner, C. A., Paron, I., Nagaraj, N. and Mann, M.** (2014). Accurate
572 Proteome-wide Label-free Quantification by Delayed Normalization and Maximal
573 Peptide Ratio Extraction, Termed MaxLFQ. *Mol Cell Proteomics* **13**, 2513–2526.
- 574 **Crocker, D., Williams, J., Costa, D. and Le Boeuf, B.** (2001). Maternal Traits and Reproductive
575 Effort in Northern Elephant Seals. *Ecology (Washington D C)* **82**, 3541–3555.
- 576 **Crocker, D. E., Khudyakov, J. I. and Champagne, C. D.** (2016). Oxidative stress in northern
577 elephant seals: Integration of omics approaches with ecological and experimental
578 studies. *Comparative Biochemistry and Physiology Part A: Molecular & Integrative*
579 *Physiology* **200**, 94–103.
- 580 **Davis, R. W.** (2014). A review of the multi-level adaptations for maximizing aerobic dive
581 duration in marine mammals: from biochemistry to behavior. *J Comp Physiol B* **184**, 23–
582 53.
- 583 **de Hoon, M. J. L., Imoto, S., Nolan, J. and Miyano, S.** (2004). Open source clustering software.
584 *Bioinformatics* **20**, 1453–1454.
- 585 **Elsner, R.** (1999). Living in water : solution to physiological problems.
- 586 **Elsner, R. and Gooden, B.** (1983). Diving and asphyxia. A comparative study of animals and
587 man. *Monogr Physiol Soc* **40**, 1–168.
- 588 **Favorit, V., Hood, W. R., Kavazis, A. N., Villamediana, P., Yap, K. N., Parry, H. A. and Skibieli, A.**
589 **L.** (2021). Mitochondrial Bioenergetics of Extramammary Tissues in Lactating Dairy
590 Cattle. *Animals* **11**, 2647.
- 591 **Geiseler, S. J., Blix, A. S., Burns, J. M. and Folkow, L. P.** (2013). Rapid postnatal development of
592 myoglobin from large liver iron stores in hooded seals. *J Exp Biol* **216**, 1793–1798.
- 593 **Gittleman, J. L. and Thompson, S. D.** (1988). Energy Allocation in Mammalian Reproduction1.
594 *American Zoologist* **28**, 863–875.
- 595 **Granger, D. N.** (1988). Role of xanthine oxidase and granulocytes in ischemia-reperfusion injury.
596 *American Journal of Physiology-Heart and Circulatory Physiology* **255**, H1269–H1275.

- 597 **Granger, D. N. and Kvietys, P. R.** (2015). Reperfusion injury and reactive oxygen species: The
598 evolution of a concept. *Redox Biology* **6**, 524–551.
- 599 **Gutgesell, A., Ringseis, R., Schmidt, E., Brandsch, C., Stangl, G. I. and Eder, K.** (2009).
600 Downregulation of peroxisome proliferator-activated receptor α and its coactivators in
601 liver and skeletal muscle mediates the metabolic adaptations during lactation in mice.
- 602 **Hille, R. and Nishino, T.** (1995). Xanthine oxidase and xanthine dehydrogenase. *The FASEB*
603 *Journal* **9**, 995–1003.
- 604 **Hindell, M., Slip, D. and Burton, H.** (1991). The Diving Behavior of Adult Male and Female
605 Southern Elephant Seals, *Mirounga-Leonina* (Pinnipedia, Phocidae). *Australian Journal*
606 *of Zoology* **39**, 595–619.
- 607 **Johnson, P., Elsner, R. and Zenteno-Savín, T.** (2004). Hypoxia-Inducible Factor in ringed seal
608 (*Phoca hispida*) tissues. *Free Radic Res* **38**, 847–854.
- 609 **Johnson, P., Elsner, R. and Zenteno-Savín, T.** (2005). Hypoxia-inducible factor 1 proteomics and
610 diving adaptations in ringed seal. *Free Radic Biol Med* **39**, 205–212.
- 611 **Kanatous, S., Davis, R., Watson, R., Polasek, L., Williams, T. and Mathieu-Costello, O.** (2003).
612 Aerobic capacities in the skeletal muscles of Weddell seals: Key to longer dive
613 durations? *The Journal of experimental biology* **205**, 3601–8.
- 614 **Kanatous, S. B., Hawke, T. J., Trumble, S. J., Pearson, L. E., Watson, R. R., Garry, D. J.,**
615 **Williams, T. M. and Davis, R. W.** (2008). The ontogeny of aerobic and diving capacity in
616 the skeletal muscles of Weddell seals. *J Exp Biol* **211**, 2559–2565.
- 617 **Kanehisa, M. and Sato, Y.** (2019). KEGG Mapper for inferring cellular functions from protein
618 sequences. *Protein Science* **29**,.
- 619 **Khudyakov, J. I., Holser, R. R., Vierra, C. A., Ly, S. T., Niel, T. K., Hasan, B. M., Crocker, D. E. and**
620 **Costa, D. P.** (2022). Changes in apolipoprotein abundance dominate proteome
621 responses to prolonged fasting in elephant seals. *Journal of Experimental Biology* **225**,
622 jeb243572.
- 623 **Kooyman, G. L.** (2012). *Diverse Divers: Physiology and behavior*. Springer Science & Business
624 Media.
- 625 **Kooyman, G. L. and Ponganis, P. J.** (1998). The physiological basis of diving to depth: birds and
626 mammals. *Annu Rev Physiol* **60**, 19–32.
- 627 **LaRosa, D. A., Cannata, D. J., Arnould, J. P. Y., O’Sullivan, L. A., Snow, R. J. and West, J. M.**
628 (2012). Changes in muscle composition during the development of diving ability in the
629 Australian fur seal. *Aust. J. Zool.* **60**, 81–90.
- 630 **Lavigne, D., Innes, S., Worthy, G., Kovacs, K., Schmitz, O. and Hickie, J.** (1986). Metabolic rate
631 of seals and whales. *Canadian Journal of Zoology* **64**, 279–284.

- 632 **Levine, R. L., Williams, J. A., Stadtman, E. P. and Shacter, E.** (1994). [37] Carbonyl assays for
633 determination of oxidatively modified proteins. In *Methods in Enzymology*, pp. 346–357.
634 Academic Press.
- 635 **Lou, R., Cao, Y., Li, S., Lang, X., Li, Y., Zhang, Y. and Shui, W.** (2023). Benchmarking commonly
636 used software suites and analysis workflows for DIA proteomics and
637 phosphoproteomics. *Nat Commun* **14**, 94.
- 638 **McCord, J. M.** (1985). Oxygen-Derived Free Radicals in Postischemic Tissue Injury. *New England*
639 *Journal of Medicine* **312**, 159–163.
- 640 **Meier, F., Brunner, A.-D., Koch, S., Koch, H., Lubeck, M., Krause, M., Goedecke, N., Decker, J.,**
641 **Kosinski, T., Park, M. A., et al.** (2018). Online Parallel Accumulation–Serial
642 Fragmentation (PASEF) with a Novel Trapped Ion Mobility Mass Spectrometer*.
643 *Molecular & Cellular Proteomics* **17**, 2534–2545.
- 644 **Meier, F., Brunner, A.-D., Frank, M., Ha, A., Bludau, I., Voytik, E., Kaspar-Schoenefeld, S.,**
645 **Lubeck, M., Raether, O., Bache, N., et al.** (2020). diaPASEF: parallel accumulation-serial
646 fragmentation combined with data-independent acquisition. *Nat Methods* **17**, 1229–
647 1236.
- 648 **Meir, J. U., Champagne, C. D., Costa, D. P., Williams, C. L. and Ponganis, P. J.** (2009). Extreme
649 hypoxemic tolerance and blood oxygen depletion in diving elephant seals. *Am J Physiol*
650 *Regul Integr Comp Physiol* **297**, R927–939.
- 651 **Modig, A., Engström, H. and Arnbom, T.** (1997). Postweaning behaviour in pups of the
652 southern elephant seal (*Mirounga leonina*) on South Georgia. *Can. J. Zool.* **75**, 582–588.
- 653 **Monaghan, P., Metcalfe, N. B. and Torres, R.** (2009). Oxidative stress as a mediator of life
654 history trade-offs: mechanisms, measurements and interpretation. *Ecology Letters* **12**,
655 75–92.
- 656 **Moore, C. D., Crocker, D. E., Fahlman, A., Moore, M. J., Willoughby, D. S., Robbins, K. A.,**
657 **Kanatous, S. B. and Trumble, S. J.** (2014). Ontogenetic changes in skeletal muscle fiber
658 type, fiber diameter and myoglobin concentration in the Northern elephant seal
659 (*Mirounga angustirostris*). *Front Physiol* **5**, 217.
- 660 **Mungai, P. T., Waypa, G. B., Jairaman, A., Prakriya, M., Dokic, D., Ball, M. K. and Schumacker,**
661 **P. T.** (2011). Hypoxia triggers AMPK activation through reactive oxygen species-
662 mediated activation of calcium release-activated calcium channels. *Mol Cell Biol* **31**,
663 3531–3545.
- 664 **Murphy, B. J. and Hochachka, P. W.** (1981). Free amino acid profiles in blood during diving and
665 recovery in the Antarctic Weddell seal. *Can. J. Zool.* **59**, 455–459.
- 666 **Noren, S., Iverson, S. and Boness, D.** (2005). Development of the Blood and Muscle Oxygen
667 Stores in Gray Seals (*Halichoerus grypus*): Implications for Juvenile Diving Capacity and
668 the Necessity of a Terrestrial Postweaning Fast. *Physiological and biochemical zoology* :
669 *PBZ* **78**, 482–90.

- 670 **Page, R. D.** (1996). TreeView: an application to display phylogenetic trees on personal
671 computers. *Comput Appl Biosci* **12**, 357–358.
- 672 **Perez-Riverol, Y., Bai, J., Bandla, C., García-Seisdedos, D., Hewapathirana, S., Kamatchinathan,**
673 **S., Kundu, D. J., Prakash, A., Frericks-Zipper, A., Eisenacher, M., et al.** (2022). The PRIDE
674 database resources in 2022: a hub for mass spectrometry-based proteomics evidences.
675 *Nucleic Acids Res* **50**, D543–D552.
- 676 **Pfaffl, M. W.** (2001). A new mathematical model for relative quantification in real-time RT-
677 PCR. *Nucleic Acids Res* **29**, e45.
- 678 **Pfleger, J., He, M. and Abdellatif, M.** (2015). Mitochondrial complex II is a source of the reserve
679 respiratory capacity that is regulated by metabolic sensors and promotes cell survival.
680 *Cell Death Dis* **6**, e1835–e1835.
- 681 **Piot, E., Hippauf, L., Charlanne, L., Picard, B., Badaut, J., Gilbert, C. and Guinet, C.** (2024). From
682 land to ocean: One month for southern elephant seal pups to acquire aquatic skills prior
683 to their first departure to sea. *Physiol Behav* **279**, 114525.
- 684 **Piotrowski, E. R., Tift, M. S., Crocker, D. E., Pearson, A. B., Vázquez-Medina, J. P., Keith, A. D.**
685 **and Khudyakov, J. I.** (2021). Ontogeny of Carbon Monoxide-Related Gene Expression in
686 a Deep-Diving Marine Mammal. *Front Physiol* **12**, 762102.
- 687 **Prewitt, J. S., Freistroffer, D. V., Schreer, J. F., Hammill, M. O. and Burns, J. M.** (2010).
688 Postnatal development of muscle biochemistry in nursing harbor seal (*Phoca vitulina*)
689 pups: limitations to diving behavior? *J Comp Physiol B* **180**, 757–766.
- 690 **Qvist, J., Hill, R. D., Schneider, R. C., Falke, K. J., Liggins, G. C., Guppy, M., Elliot, R. L.,**
691 **Hochachka, P. W. and Zapol, W. M.** (1986). Hemoglobin concentrations and blood gas
692 tensions of free-diving Weddell seals. *J Appl Physiol (1985)* **61**, 1560–1569.
- 693 **R Core Team** R: a language and environment for statistical computing. R Foundation for
694 Statistical Computing, Vienna, Austria. URL <https://www.R-project.org/>. 2022.
- 695 **Ridgway, S. H., Harrison, R. J. and Joyce, P. L.** (1975). Sleep and cardiac rhythm in the gray seal.
696 *Science* **187**, 553–555.
- 697 **Rivett, A. J.** (1985). Preferential degradation of the oxidatively modified form of glutamine
698 synthetase by intracellular mammalian proteases. *Journal of Biological Chemistry* **260**,
699 300–305.
- 700 **Roberts, L. J. and Morrow, J. D.** (2000). Measurement of F2-isoprostanes as an index of
701 oxidative stress in vivo. *Free Radical Biology and Medicine* **28**, 505–513.
- 702 **Schiaffino, S. and Reggiani, C.** (1994). Myosin isoforms in mammalian skeletal muscle. *J Appl*
703 *Physiol (1985)* **77**, 493–501.
- 704 **Sert, N. P. du, Hurst, V., Ahluwalia, A., Alam, S., Avey, M. T., Baker, M., Browne, W. J., Clark,**
705 **A., Cuthill, I. C., Dirnagl, U., et al.** (2020). The ARRIVE guidelines 2.0: Updated guidelines
706 for reporting animal research. *PLOS Biology* **18**, e3000410.

- 707 **Sharick, J. T., Vazquez-Medina, J. P., Ortiz, R. M. and Crocker, D. E.** (2015). Oxidative stress is a
708 potential cost of breeding in male and female northern elephant seals. *Functional*
709 *Ecology* **29**, 367–376.
- 710 **Slip, D. J., Hindell, M. A. and Burton, H. R.** (1994). Fourteen. Diving behavior of southern
711 elephant seals from Macquarie island: an overview. In *Elephant Seals* (ed. Le Boeuf, B.
712 J.) and Laws, R. M.), pp. 253–270. University of California Press.
- 713 **Somo, D. A., Ensminger, D. C., Sharick, J. T., Kanatous, S. B. and Crocker, D. E.** (2015).
714 Development of Dive Capacity in Northern Elephant Seals (*Mirounga angustirostris*):
715 Reduced Body Reserves at Weaning Are Associated with Elevated Body Oxygen Stores
716 during the Postweaning Fast. *Physiological and Biochemical Zoology* **88**, 471–482.
- 717 **Soñanez-Organis, J. G., Vázquez-Medina, J. P., Crocker, D. E. and Ortiz, R. M.** (2013).
718 Prolonged fasting activates hypoxia inducible factor -1 α , -2 α and -3 α in a tissue-specific
719 manner in northern elephant seal pups. *Gene* **526**, 155–163.
- 720 **Speakman, J. R. and Garratt, M.** (2014). Oxidative stress as a cost of reproduction: Beyond the
721 simplistic trade-off model. *BioEssays* **36**, 93–106.
- 722 **Tadaishi, M., Miura, S., Kai, Y., Kano, Y., Oishi, Y. and Ezaki, O.** (2011). Skeletal Muscle-Specific
723 Expression of PGC-1 α -b, an Exercise-Responsive Isoform, Increases Exercise Capacity
724 and Peak Oxygen Uptake. *PLOS ONE* **6**, e28290.
- 725 **Talmadge, R. J. and Roy, R. R.** (1993). Electrophoretic separation of rat skeletal muscle myosin
726 heavy-chain isoforms. *Journal of Applied Physiology* **75**, 2337–2340.
- 727 **Thorson, P. H. and Le Boeuf, B. J. L.** (2023). Fifteen. Developmental aspects of diving in
728 northern elephant seal pups. In *Fifteen. Developmental aspects of diving in northern*
729 *elephant seal pups*, pp. 271–289. University of California Press.
- 730 **Tyanova, S., Temu, T. and Cox, J.** (2016). The MaxQuant computational platform for mass
731 spectrometry-based shotgun proteomics. *Nat Protoc* **11**, 2301–2319.
- 732 **Vázquez-Medina, J. P., Zenteno-Savín, T. and Elsner, R.** (2006). Antioxidant enzymes in ringed
733 seal tissues: Potential protection against dive-associated ischemia/reperfusion.
734 *Comparative Biochemistry and Physiology Part C: Toxicology & Pharmacology* **142**, 198–
735 204.
- 736 **Vázquez-Medina, J. P., Zenteno-Savin, T. and Elsner, R.** (2007). Glutathione protection against
737 dive-associated ischemia/reperfusion in ringed seal tissues. *Journal of Experimental*
738 *Marine Biology and Ecology* **345**, 110–118.
- 739 **Vázquez-Medina, J. P., Crocker, D. E., Forman, H. J. and Ortiz, R. M.** (2010). Prolonged fasting
740 does not increase oxidative damage or inflammation in postweaned northern elephant
741 seal pups. *Journal of Experimental Biology* **213**, 2524–2530.
- 742 **Vázquez-Medina, J. P., Zenteno-Savín, T., Forman, H. J., Crocker, D. E. and Ortiz, R. M.**
743 (2011a). Prolonged fasting increases glutathione biosynthesis in postweaned northern
744 elephant seals. *Journal of Experimental Biology* **214**, 1294–1299.

- 745 **Vázquez-Medina, J. P., Soñanez-Organis, J. G., Burns, J. M., Zenteno-Savín, T. and Ortiz, R. M.**
 746 (2011b). Antioxidant capacity develops with maturation in the deep-diving hooded seal.
 747 *J Exp Biol* **214**, 2903–2910.
- 748 **Vázquez-Medina, J. P., Zenteno-Savín, T., Tift, M. S., Forman, H. J., Crocker, D. E. and Ortiz, R.**
 749 **M.** (2011c). Apnea stimulates the adaptive response to oxidative stress in elephant seal
 750 pups. *Journal of Experimental Biology* **214**, 4193–4200.
- 751 **Weir, H. J., Yao, P., Huynh, F. K., Escoubas, C. C., Goncalves, R. L., Burkewitz, K., Laboy, R.,**
 752 **Hirschey, M. D. and Mair, W. B.** (2017). Dietary Restriction and AMPK Increase Lifespan
 753 via Mitochondrial Network and Peroxisome Remodeling. *Cell Metab* **26**, 884-896.e5.
- 754 **Wilhelm Filho, D., Sell, F., Ribeiro, L., Ghislandi, M., Carrasquedo, F., Fraga, C. G., Wallauer, J.**
 755 **P., Simões-Lopes, P. C. and Uhart, M. M.** (2002). Comparison between the antioxidant
 756 status of terrestrial and diving mammals. *Comp Biochem Physiol A Mol Integr Physiol*
 757 **133**, 885–892.
- 758 **Wright, T. J., Davis, R. W., Holser, R. R., Hückstädt, L. A., Danesi, C. P., Porter, C., Widen, S. G.,**
 759 **Williams, T. M., Costa, D. P. and Sheffield-Moore, M.** (2020). Changes in Northern
 760 Elephant Seal Skeletal Muscle Following Thirty Days of Fasting and Reduced Activity.
 761 *Front. Physiol.* **11**, 564555.
- 762 **Xiao, X. Q., Grove, K. L. and Smith, M. S.** (2004). Metabolic Adaptations in Skeletal Muscle
 763 during Lactation: Complementary Deoxyribonucleic Acid Microarray and Real-Time
 764 Polymerase Chain Reaction Analysis of Gene Expression. *Endocrinology* **145**, 5344–5354.
- 765 **Zenteno-Savín, T., Clayton-Hernández, E. and Elsner, R.** (2002). Diving seals: are they a model
 766 for coping with oxidative stress? *Comp Biochem Physiol C Toxicol Pharmacol* **133**, 527–
 767 536.

768

769 **Figure legends**

770

771 **Figure 1.** Mitochondrial respiratory flux in juvenile (N = 5) and adult (N = 6) southern elephant seals's
 772 muscle: A. Protocol A (fatty acids). B. Protocol B (carbohydrates) and respiratory ratios (C. Protocol A, D.
 773 Protocol B). Ratios of respiratory rates were calculated to assess the OXPHOS coupling control factor,
 774 calculated as $(OXPHOS_{Cl-LEAK})/OXPHOS_{Cl}$, the contribution of Complex I+II coupled respiration to
 775 Maximal non-coupled Complex I+II respiration ($OXPHOS_{Cl+ClII}/MAX_{Cl+ClII}$), and the relative contribution of
 776 Maximal non-coupled Complex II respiration capacity to Maximal non-coupled Complex I+II respiration
 777 ($MAX_{ClII}/MAX_{Cl+ClII}$). Statistical significance (* $p < 0.05$, Wilcoxon test). Results are expressed as
 778 mean \pm standard error.

779

780 **Figure 2.** Overview of SES muscle proteomic between juvenile and adult SES. Changes in the proteome
 781 of the *longissimus dorsi* muscle between juveniles (N = 5) and adults (N = 6) are shown as heat maps of

782 differentially expressed proteins that were produced by hierarchical clustering (A). Signal values
783 between groups were successfully discriminated (green, black, and red boxes represent downregulated,
784 intermediate, and upregulated proteins, respectively). Functional annotation analysis from differential
785 proteins revealed enriched Gene Ontology terms, which allowed the determination of broad functions
786 significantly affected by age, i.e., regular exposition to stressful events, physical activity, fasting (B; filled
787 circles represent the broad functions depicted by proteins that are discussed in this paper).

788

789 **Figure 3.** Regulation of key metabolic pathways in the *longissimus dorsi* muscle of juveniles (N = 5) and
790 adult SES (N = 6). The relative abundance is shown using the following color code: significantly (Welch
791 student and paired Student tests; P < 0.05) up-regulated proteins in juveniles are shown in dark orange
792 boxes with white text. Down-regulated proteins in juveniles are in light orange boxes with black text.
793 Blue boxes show proteins that did not change, and black boxes show undetected proteins. (A)
794 Mitochondrial pathways. (B) Schematic representation of the proposed mechanisms that activate
795 protective responses to oxidative stress, hypoxia, calorie restriction, and / or physical activity.

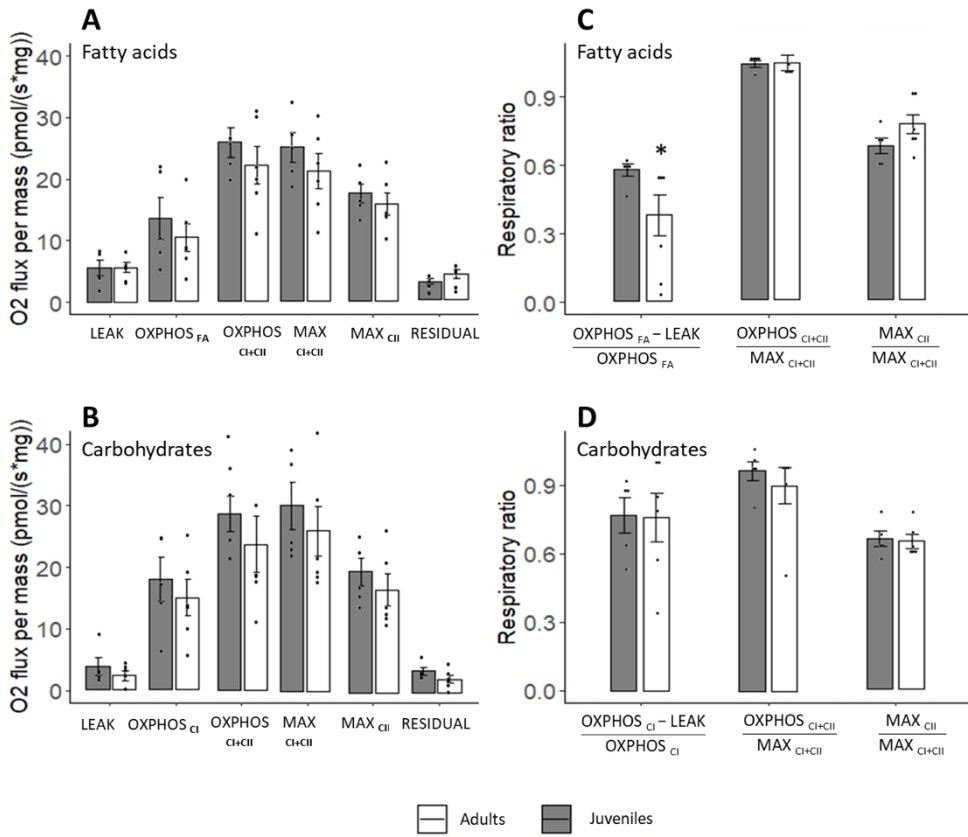
796

797 **Figure 4:** cellular oxidative damage in adult (N = 6) and juvenile (N = 5) female southern elephant seals.
798 (A) plasma concentration of isoprostanes (8-isoPGF2 α). (B) Plasma concentration of protein carbonyls
799 (nmol per mg proteins). No difference was observed in either 8-isoPGF2a (Wilcoxon test, W = 7, p-value
800 = 0.18) or protein carbonyls (Wilcoxon test, W = 15, p-value = 1.0). Results are expressed as
801 mean \pm standard error.

802

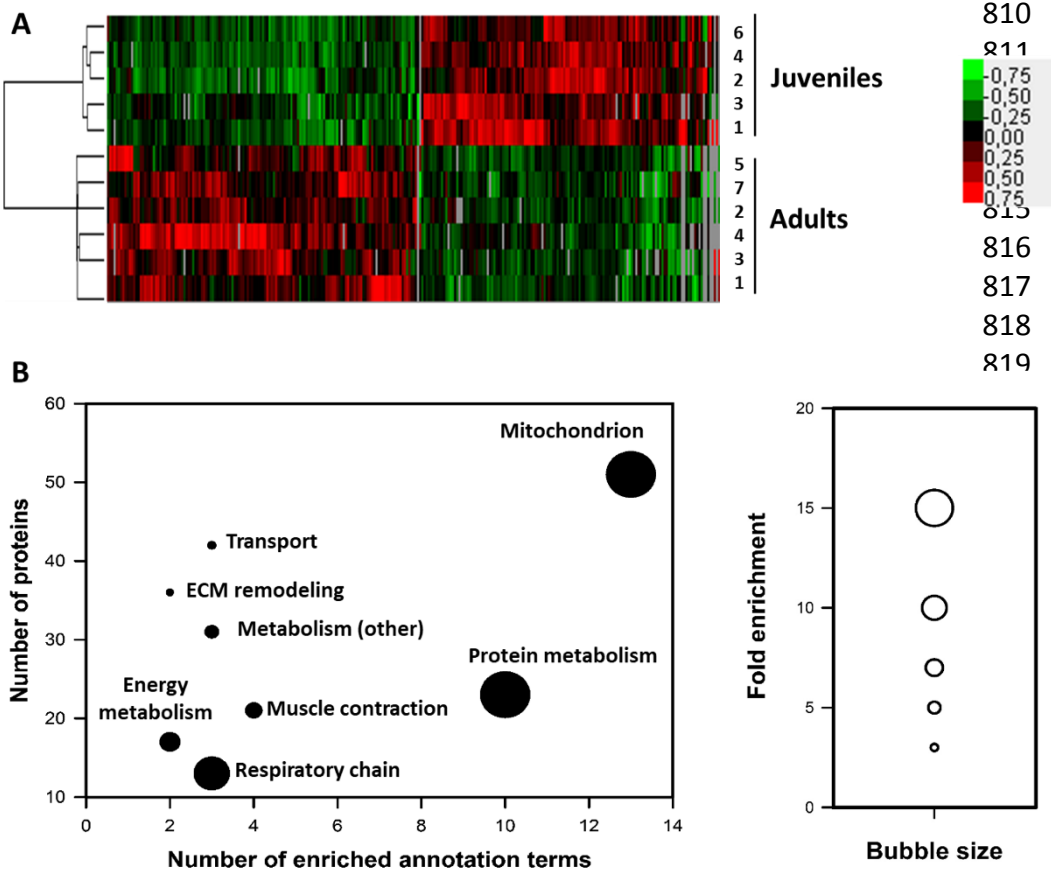
803

804



805
806
807
808
809

Figure 1



810
811
812
813
814
815
816
817
818
819

832

833

834 **Figure 2**

835

836

837

838

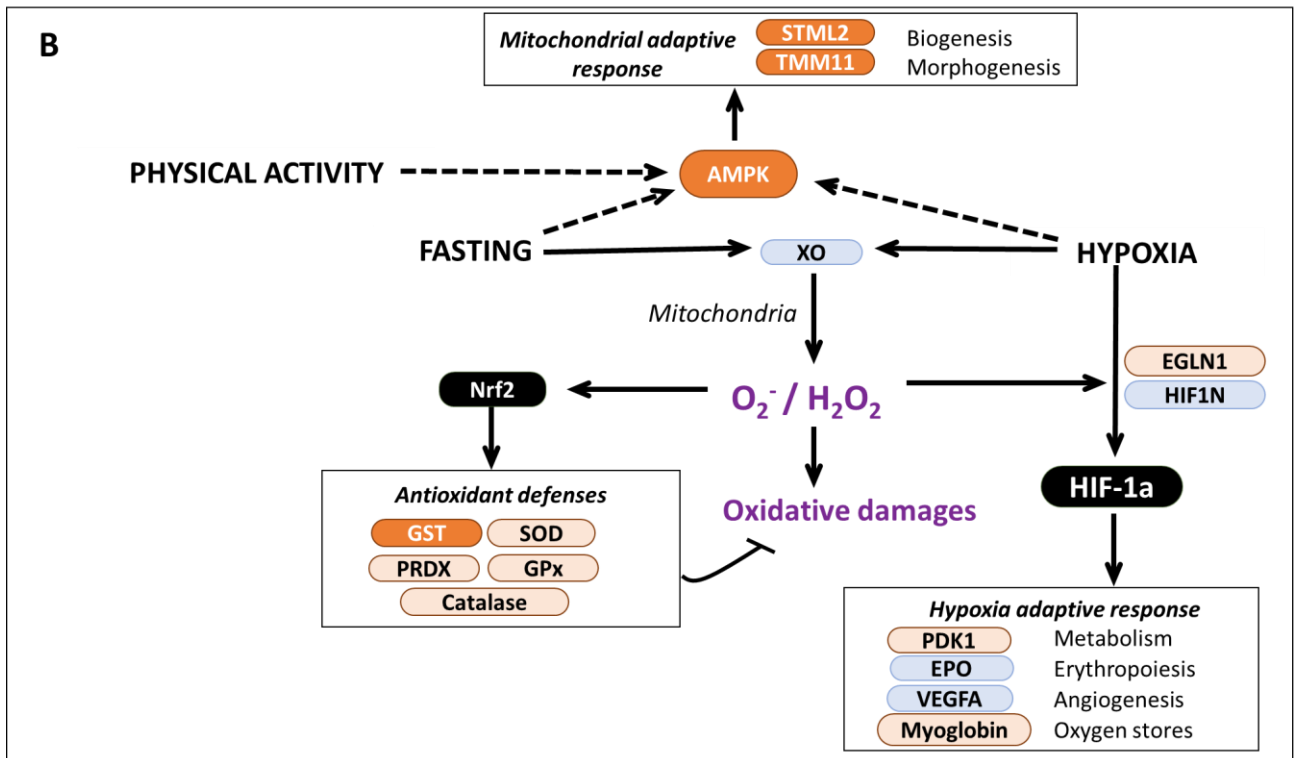
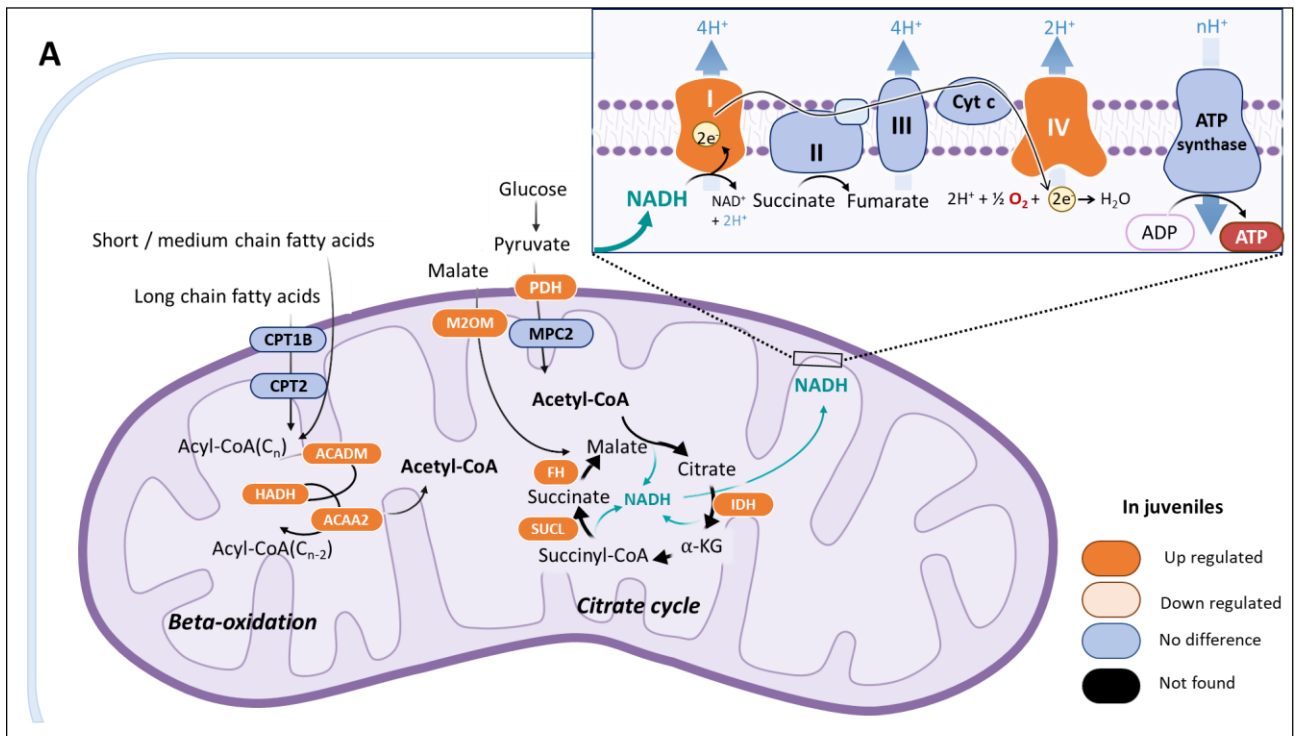
839

840 **Figure 3**

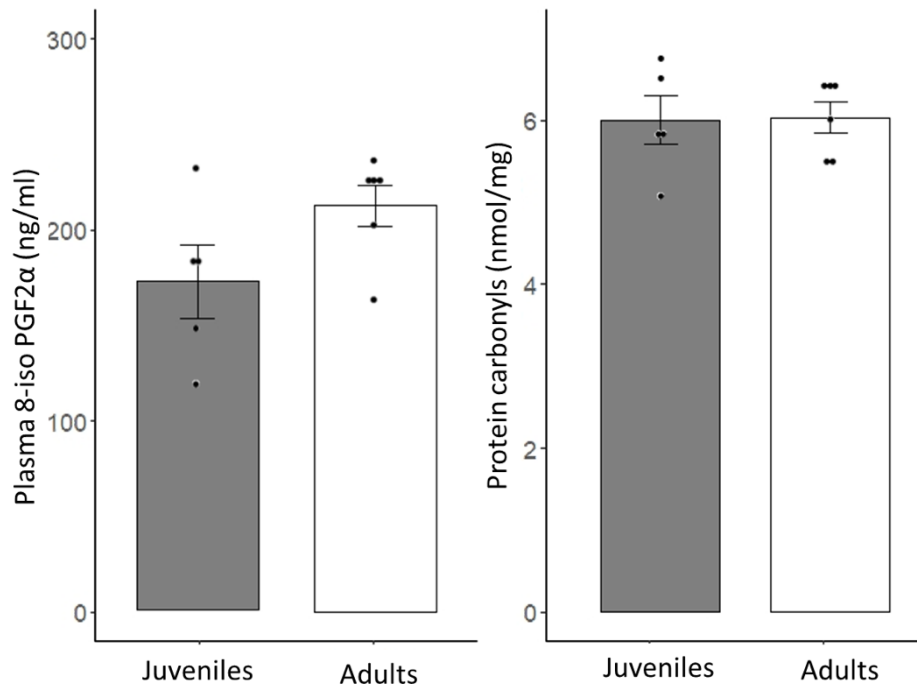
841

842

843



844
845
846
847
848
849
850



851

852

853

854

855

856 **Figure 4**

857

858

859

860

861

862

863

864

865